Lung-Cancer Risk in Mice after Exposure to Gamma Rays, Carbon Ions or Neutrons: Egfr Pathway Activation and Frequent Nuclear Abnormality

Authors: Suzuki, Kenshi, Yamazaki, Shunsuke, Iwata, Ken-ichi, Yamada, Yutaka, Morioka, Takamitsu, et al.

Source: Radiation Research, 198(5) : 475-487

Published By: Radiation Research Society

URL: https://doi.org/10.1667/RADE-21-00192.1

RADIATION RESEARCH **198**, 475–487 (2022)
0033-7587/22 $15.00

DOI: 10.1667/RADE-21-00192.1

Lung-Cancer Risk in Mice after Exposure to Gamma Rays, Carbon Ions or Neutrons: Egfr Pathway Activation and Frequent Nuclear Abnormality

Kenshi Suzuki, Shunsuke Yamazaki, Ken-ichi Iwata, Yutaka Yamada, Takamitsu Morioka, Kazuhiro Daino, Mutsumi Kaminishi, Mari Ogawa, Yoshiya Shimada[1] and Shizuko Kakinuma[2]

Department of Radiation Effects Research, National Institute of Radiological Sciences (NIRS), National Institutes for Quantum Science and Technology (QST), Chiba, Japan

Suzuki K, Yamazaki S, Iwata K, Yamada Y, Morioka T, Daino K, Kaminishi M, Ogawa M, Shimada Y. Kakinuma S. Lung-Cancer Risk in Mice after Exposure to Gamma Rays, Carbon Ions or Neutrons: Egfr Pathway Activation and Frequent Nuclear Abnormality. Radiat. Res. 198, 475–487 (2022).

Lung is one of the high-risk organs for radiation-induced carcinogenesis, but the risk of secondary lung-cancer development after particle-beam therapy and the underlying mechanism(s) remain to be elucidated. To investigate the effects of particle-beam radiation on adjacent normal tissues during cancer therapy, 7-week-old male and female B6C3F1 mice were irradiated with 0.2–4 Gy of gamma rays (for comparison), carbon ions (290 MeV/u, linear energy transfer 13 keV/μm), or fast neutrons (0.05–1 Gy, mean energy, ~2 MeV), and lung-tumor development was assessed by histopathology. Mice irradiated with ≥2 Gy of carbon ions or ≥0.2 Gy of neutrons developed lung adenocarcinoma (AC) significantly sooner than did non-irradiated mice. The relative biological effectiveness values for carbon ions for lung AC development were 1.07 for male mice and 2.59 for females, and the corresponding values for neutrons were 4.63 and 4.57. Genomic analysis of lung ACs revealed alterations in genes involved in Egfr signaling. Hyperphosphorylation of Erk and a frequent nuclear abnormality (i.e., nuclear groove) were observed in lung ACs of mice irradiated with carbon ions or neutrons compared with ACs from non-irradiated or gamma-ray-irradiated groups. Our data indicate that the induction of lung AC by carbon ions occurred at a rate similar to that for gamma rays in males and approximately 2- to 3-fold greater than that for gamma rays in females. In contrast, the effect of neutrons on lung AC development was approximately 4- to 5-fold greater than that of gamma rays. Our results provide valuable information concerning risk assessment of radiation-induced lung tumors after particle-beam therapy and increase our understanding of the molecular basis of tumor development.

Editor's note. The online version of this article (DOI: https://doi.org/10.1667/RADE-21-00192.1) contains supplementary information that is available to all authorized users.

[1] Current address: Institute for Environmental Sciences, Ienomae, Obuchi, Rokkashomura 039-3212, Japan.

[2] Corresponding Author: 4-9-1, Anagawa, Inage-ku, Chiba, 263-8555, Japan; email: kakinuma.shizuko@qst.go.jp.

INTRODUCTION

Recent advances in radiation therapy technology have resulted in an increased number of cancer patients undergoing radiation therapy (*1*). The use of particle-beam therapy with protons or carbon ions has increased rapidly worldwide because of the enhanced ability to deliver the dose directly to tumors, thereby reducing the dose to adjacent normal tissues (*2*). During carbon-ion therapy, however, normal tissues surrounding a tumor may be exposed to carbon ions with a linear energy transfer (LET) of 13 keV/μm (*3*). During carbon-ion therapy, incident carbon particles form the Bragg peak and reach their maximum effect at a specific subdermal depth inside the body. On the other hand, particles with energy of 13 keV pass through the normal tissues around the tumor. Thus, it is necessary to evaluate the risk of secondary cancer after carbon-ion therapy at this LET. In addition, particle-beam therapy generates neutrons as secondary particles that potentially could damage DNA in healthy cells (*4, 5*). These issues raise concerns about the potential increased risk of developing radiation-induced secondary cancers.

Lung cancer accounts for the greatest number of cancer-related deaths worldwide (*6, 7*). Although the radiosensitivity of an organ depends on the distribution of stem cells and tissue-specific repair mechanisms, the lung is considered a high-risk organ for radiation carcinogenesis because of its very large surface area, which increases the likelihood that cellular DNA may undergo mutation after exposure to various potential environment carcinogens, including ionizing radiation. In fact, radiation exposure increases the risk of developing lung cancer, as revealed by epidemiological studies of Japanese atomic bomb survivors (*8, 9*), patients who have received radiotherapy (*10*), and people exposed to alpha particles via inhalation of radon-222 (*11, 12*). Moreover, radiation therapy for breast-cancer patients

increases the risk of developing secondary lung cancer (*13*). Based on tumor histology, lung cancer is classified into three types, namely adenocarcinoma (AC), squamous-cell carcinoma, and small-cell carcinoma. Studies of lung-cancer prevalence in the atomic-bomb survivors revealed radiation-associated increases in the relative risk for developing all three major types of lung cancer (*14, 15*).

Epidemiological studies provide important information for estimating cancer risk after radiation therapy. However, the lifestyles and daily habits of people (e.g., diet, smoking history) can confound the estimation of risk. In this regard, animal experiments are useful for studying the risks and mechanisms of cancer development because the effects of potential confounding factors can be minimized. Large-scale animal experiments using mice have been conducted to examine life shortening and radiation-induced carcinogenesis after exposure to gamma rays or fission neutrons, revealing an increased risk of developing lung cancer (*16, 17*). Molecular analyses have revealed genetic alterations in the tumor-suppressor genes *Rb* and *Trp53* and oncogene *Kras* in lung cancers from irradiated and control mice (*18, 19*). These data demonstrate that radiation carcinogenesis experiments with mice can enhance our ability to assess the risk of developing lung cancer after radiation exposure and help us understand the underlying mechanisms.

To the best of our knowledge, no study has examined the risk and pathological and molecular biological aspects of lung cancer caused by exposure to carbon ions or neutrons. To address this deficient, we evaluated the risk of lung-cancer development (and the underlying mechanisms) in male and female mice exposed to carbon ions or neutrons in comparison with non-irradiated-control mice or gamma-irradiated.

MATERIALS AND METHODS

Tumor Samples

B6C3F1 mice were generated by crossing male C57BL/6NCrlCrlj and female C3H/HeNCrlCrlj mice, both of which were purchased from Charles River (Kanagawa, Japan). The mice were bred in a specific pathogen-free environment under the following conditions: 12 h light/dark cycle, 23 ± 2°C, and 50 ± 10% humidity. Mice were fed a standard laboratory chow (MBR-1 Funabashi Farm, Chiba, Japan) and provided with water ad libitum. At 7 weeks of age, mice were either not irradiated (control) or subjected to whole-body irradiation with gamma rays, carbon ions or neutrons. Mice were observed daily until they became moribund (drastic weight loss or weakness) or died, and all moribund mice were euthanized by phlebotomy under isoflurane and subjected to necroscopy. Lungs and other organs were removed at autopsy to assess lung-cancer development and metastasis. All cancerous lung lesions and normal tissues, including lung, ear, and tail, were immediately frozen in liquid nitrogen for molecular analysis. A part of the lung lesions and normal tissues were then fixed in 10% neutral buffered formalin and embedded in paraffin for histopathological diagnosis. All experimental protocols were reviewed and approved by the Institutional Animal Care and Use Committee of the National Institute of Radiological Sciences (NIRS; approval no. 07-1017) and performed in strict accordance with the NIRS Guide for Care and Use of Laboratory Animals.

TABLE 1
Incidence of Lung Tumors in Non-Irradiated (Control) and Irradiated Mice

Group	Dose (Gy)	Sex	No. of animals	No. of AD (%)	No. of AC (%)
Control	0	M	111	14 (12.6)	10 (9)
		F	108	7 (6.5)	4 (3.7)
Gamma rays	0.2	M	51	5 (9.8)	9 (17.6)
		F	51	3 (5.9)	2 (3.9)
	0.5	M	50	3 (6)	3 (6)
		F	50	0 (0)	1 (2)
	1	M	50	3 (6)	7 (14)
		F	50	3 (6)	3 (6)
	2	M	51	3 (5.9)	8 (15.7)
		F	51	5 (9.8)	6 (11.8)
	4	M	50	1 (2)	7 (14)
		F	50	2 (4)	1 (2)
Carbon ions	0.2	M	43	1 (2.3)	5 (11.6)
		F	36	1 (2.8)	7 (19.4)
	0.5	M	40	2 (5)	3 (7.5)
		F	41	3 (7.3)	2 (4.9)
	1	M	40	4 (10)	3 (7.5)
		F	41	2 (4.9)	5 (12.2)
	2	M	41	4 (9.8)	8 (19.5)
		F	48	1 (2.1)	6 (12.5)
	4	M	40	1 (2.5)	6 (15)
		F	40	0 (0)	3 (7.5)
Neutrons[a]	0.0485	M	49	2 (4.1)	9 (18.4)
		F	50	3 (6)	2 (4)
	0.097	M	50	6 (12)	3 (6)
		F	50	1 (2)	5 (10)
	0.194	M	50	4 (8)	8 (16)
		F	50	3 (6)	5 (10)
	0.485	M	50	3 (6)	6 (12)
		F	50	2 (4)	1 (2)
	0.97	M	50	2 (4)	9 (18)
		F	50	3 (6)	3 (6)

Abbreviations: AD = adenoma, AC = adenocarcinoma; M = male, F = female.

[a] Neutron doses are shown excluding gamma contamination doses.

Irradiation

A total of 40–50 mice per group were used (Table 1) (*20*). The number of animals used was determined by validating the sample size of the COX proportional hazards model (calculated with the statistical software R) to ensure that it had sufficient detection sensitivity to calculate the Relative biological effectiveness (RBE). Mice were gamma irradiated (0.2–4 Gy) using a 57.35-TBq ^{137}Cs radiation source (Gammacell 40; Nordion International, Ontario, Canada) at an acute dose rate of 540 mGy/min. Carbon-ion irradiation (0.2–4 Gy) of mice was carried out at the HIMAC facility (*21*) at NIRS/QST using a 290-MeV/u monoenergetic carbon-ion beam (LET, 13 keV/μm). Details of the HIMAC beam delivery system, physical properties, biological irradiation procedures, and dosimetry have been reported elsewhere (*3, 21*). Mice were irradiated with fast neutrons (0.05–1 Gy) at an accelerator facility [Neutron Exposure Accelerator System for Biological Effects Experiment, (NIRS-NASBEE), Chiba, Japan]. Details of the neutron production mechanisms and dosimetry have been reported elsewhere (*22, 23*). Briefly, a beryllium target was irradiated with 4 MeV accelerated deuterons to produce fast neutrons with a major peak at 1.7 MeV and average energy of 2.3 MeV. The tissue-absorbed dose comprised 82% neutrons and 18% gamma rays,

as measured previously using neutron-sensitive and -insensitive proportional counters (*24*).

Pathological Analysis

Sections of lung lesions were prepared from formalin-fixed, paraffin-embedded tissue blocks. Each section was subjected to hematoxylin and eosin staining and scanned using a NanoZoomer 2.0-HT slide digitizer (Hamamatsu Photonics KK, Hamamatsu, Japan). Lung lesions were classified as adenoma (AD) or AC by pathologists based on the observation of an atypical nuclear morphology or cell shape. To examine the frequency of nuclear grooves in lung lesions, a total of five visual fields (~400 cells per field) were randomly selected for each lesion, and tumor cells with nuclear grooves were counted. Lung lesions were then categorized as follows: high (++), moderate (+), or low (–) incidence of nuclear grooves, if ≥50%, 10 to <50%, or <10% of tumor cells with nuclear grooves were observed in each visual field, respectively.

Loss of Heterozygosity (LOH) Analysis

Genomic DNA samples from lung AC and normal ear samples were amplified by PCR using five microsatellite simple-sequence-length polymorphism markers on chromosome 4, including the *Cdkn2b* locus, and five markers on chromosome 6, including the *Braf* locus. The PCR products were analyzed by agarose gel electrophoresis using 4% NuSieve agarose (3:1; FMC, Rockland, MA) and a capillary electrophoresis system, namely an HAD-GT12 Genetic Analyzer (eGene Inc., Irvine, CA).

Array-Comparative Genomic Hybridization (CGH) Analysis

Genomic DNAs from lung AC and normal ear samples were labeled with cyanine 3-UTP or cyanine 5-dUTP, respectively, and purified using a purification column (Agilent Technologies, Santa Clara, CA). Labeled DNAs were hybridized to microarray slides (SurePrint G3 Mouse CGH, 4 × 180K; Agilent Technologies) at 67°C with rotation at 20 rpm for 24 h. Then, slides were washed with Wash Buffers 1 and 2 (Agilent Technologies) and scanned using the Agilent G2505C microarray scanner. Scanned images were processed using Agilent Feature Extraction software (ver. 10.7.3.1), and the data were analyzed using Agilent Genomic Workbench software 7.0.4.0. The microarray data were deposited in the Gene Expression Omnibus database (www.ncbi.nlm.nih.gov/geo) under accession number GSE174131.

Gene Mutation Analysis

Mutations in *Egfr*, *Kras*, *Braf*, *Trp53*, and *Cdkn2b* were analyzed by direct sequencing of PCR products of cDNAs from lung ACs using a Model 3130 Genetic Analyzer (Applied Biosystems, Foster City, CA) and the BigDye Terminator kit (Life Technologies Inc., Carlsbad, CA). Supplementary Table S1 (https://doi.org/10.1667/RADE-21-00192.1.S1) lists primer sequences and PCR conditions. Sequence data were analyzed using ATGC and GENETYX software (Genetyx Corporation, Tokyo, Japan).

Immunostaining

Tissue sections were autoclaved in 10 mM sodium citrate (pH 6.0) at 120°C for 20 min for antigen retrieval and then incubated at 4°C overnight with a primary antibody against Erk (p44/42 MAP kinase) or phospho-Erk (1:100, Cell Signaling Technology, Danvers, MA). Sections were then incubated with a peroxide-conjugated secondary antibody (Histofine Simple Stain MAX PO, Nichirei Bio Science, Tokyo, Japan). Immunopositivity was visualized with the 3,3-Diaminobenzidine Substrate kit (Vector Laboratories, Burlingame, CA) followed by counterstaining with hematoxylin. Immunohistochemically stained samples on slides were scanned using the NanoZoomer 2.0-HT slide digitizer (Hamamatsu Photonics KK). Each image was analyzed using Tissue Studio software (CTC Life Science Co., Ltd., Tokyo, Japan). Immunopositivity for phospho-Erk was calculated by dividing the number of phospho-Erk immunopositive cells by the total number of cells in a unit area and scored as negative (–), positive (+) or highly positive (++).

Statistics

The statistical significance of differences in survival between groups was determined by the log rank test using SPSS Statistics (ver. 24; IBM, Endicott, NY). Multivariate Cox proportional hazard analysis was performed for the calculation of hazard ratios using SPSS Statistics (ver. 24). Fisher's exact probability test was performed to compare disease incidence, proportion of phospho-Erk-positive tumors, and appearance of nuclear grooves between groups. Differences were considered significant for P values of <0.05. Computations were performed using the epifit package in the statistical software R (*25*).

RESULTS

Lung Carcinogenesis in Mice after Irradiation

To understand how gamma rays, carbon ions (LET of 13 keV/μm) or neutrons (mean energy, ~2 MeV) contribute to lung tumorigenesis, male and female B6C3F1 mice were irradiated with gamma rays or carbon ions (dose range 0.2–4 Gy) or neutrons (range 0.05–1 Gy) at age 7 weeks, and the incidence of lung lesions was analyzed (Table 1). Tumor incidence did not differ significantly between male and female mice (AD, $P = 0.76$; AC, $P = 0.43$). Next, to compare the effect of the aforementioned radiation types on the incidence of lung lesions, lung lesion–free survival curves were plotted for the non-irradiated and 1 Gy irradiated groups (Fig. 1). Lung AD developed significantly earlier in the neutron-irradiated female mice compared with the control and carbon-ion irradiated groups (control vs. neutron, $P < 0.001$; carbon ion vs. neutron, $P < 0.05$) (Fig. 1C). Neutron-irradiated male mice developed lung AC significantly earlier than the other groups (control vs. neutron, $P < 0.001$; gamma ray vs. neutron; $P < 0.05$; carbon ion vs. neutron, $P < 0.05$) (Fig. 1D). Carbon-ion irradiated or neutron-irradiated female mice developed lung AC significantly earlier than the control group (control vs. neutron, $P < 0.05$; control vs. carbon ion, $P < 0.01$) (Fig. 1E). Next, we examined the radiation dose dependency of lung-lesion development among the various irradiated groups. Irradiation with gamma rays, carbon ions, or neutrons led to a significant dose-dependent increase in the incidence of lung AD in both male and female mice, and lung AD-free survival was significantly shortened in female mice irradiated with ≥2 Gy of gamma rays or 1 Gy of neutrons (Supplementary Fig. S1; https://doi.org/10.1667/RADE-21-00192.1.S2). Lung AC-free survival was significantly shortened in male mice after irradiation with ≥2 Gy of gamma rays or carbon ions or with ≥ 0.2 Gy of neutrons (Supplementary Fig. S2; https://doi.org/10.1667/RADE-21-00192.1.S2). The lung AC-free survival of female mice was significantly shortened after 2 Gy gamma irradiation, with

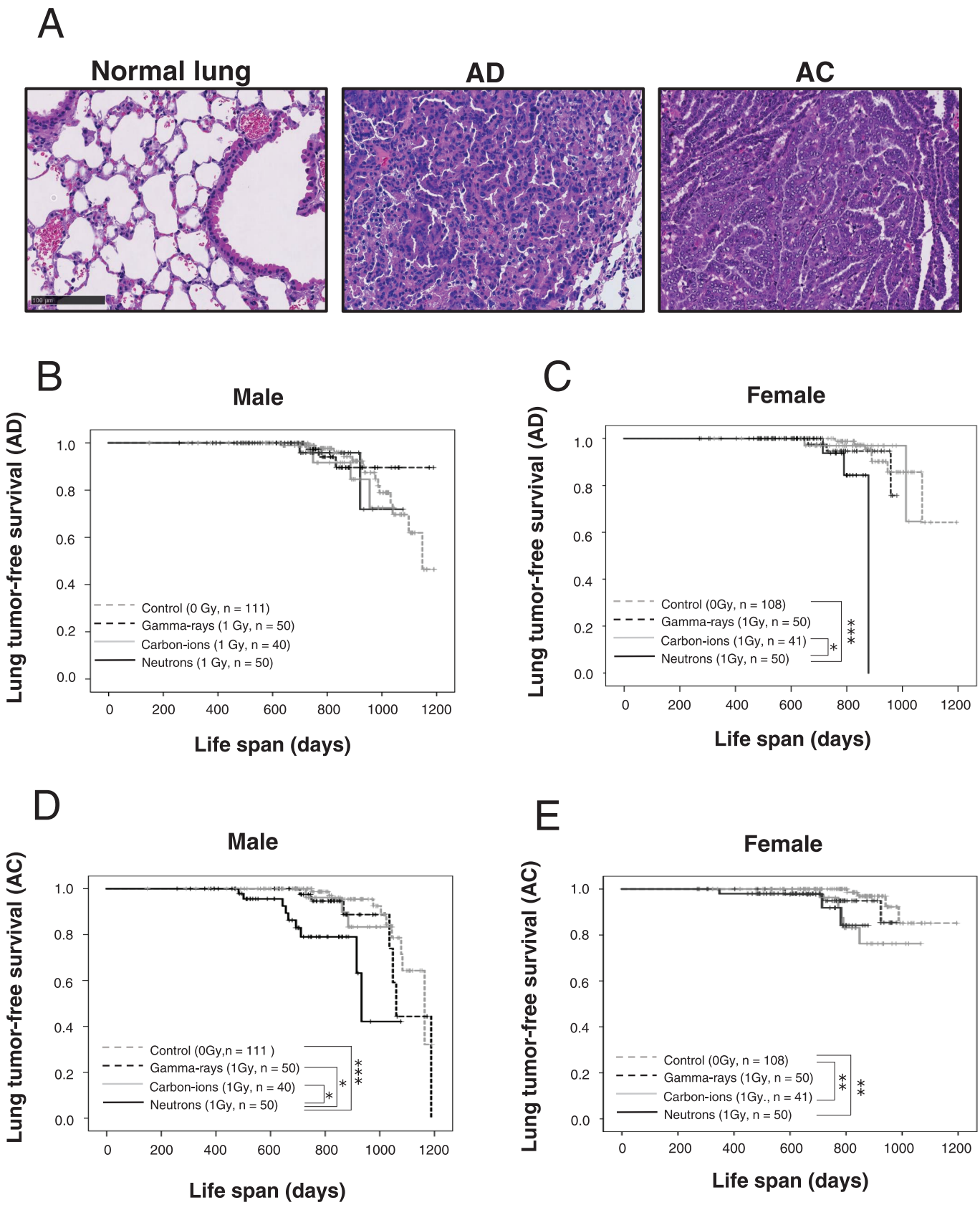

FIG. 1. Incidence of lung lesions in irradiated mice. Panel A: Representative histological images of normal lung tissue as well as AD and AC tissues of the lung. Kaplan-Meier curves for lung AD- and AC-free survival of male (panels B and D) and female (panels C and E) mice after irradiation with 1 Gy of gamma rays, carbon ions, or neutrons. Data for non-irradiated control mice are also presented. *$P < 0.05$, **$P < 0.01$ and ***$P < 0.001$.

TABLE 2
Hazard Ratio Values for the Development of Lung Lesions after Irradiation of Mice with Gamma Rays

Sex	Lung lesion	Dose (Gy)	No. of animals	P value	Hazard ratio	95% CI Lower limit	95% CI Upper limit
Male	Adenoma	0	111	0.99	1.00	-	-
		0.2	51	0.99	1.00	0.36	2.79
		0.5	50	0.69	0.77	0.22	2.72
		1	50	0.55	0.68	0.20	2.38
		2	51	0.87	0.90	0.25	3.18
		4	50	0.99	0.99	0.12	7.97
	Adenocarcinoma	0	111	0.00	1.00	-	-
		0.2	51	0.049*	2.48	1.00	6.15
		0.5	50	0.93	1.06	0.29	3.92
		1	50	0.19	1.96	0.73	5.21
		2	51	0.19	3.37	1.31	8.70
		4	50	<0.001***	10.11	3.53	28.96
Female	Adenoma	0	108	0.67	1.00	-	-
		0.2	51	0.71	0.80	0.20	3.12
		0.5	50	0.98	0.00	0.00	-
		1	50	0.45	1.65	0.41	6.67
		2	51	0.88	3.90	1.18	12.89
		4	50	0.13	2.94	0.56	15.41
	Adenocarcinoma	0	108	0.11	1.00	-	-
		0.2	51	0.81	0.83	0.15	4.64
		0.5	50	0.53	0.50	0.06	4.50
		1	50	0.14	3.00	0.65	13.81
		2	51	0.026*	6.92	1.93	24.83
		4	50	0.35	2.43	0.26	22.72

Notes. CI = confidence interval. *$P < 0.05$; ***$P < 0.001$ vs. no irradiation.

≥1 Gy of carbon ions, or with 0.2 Gy or 1 Gy of neutrons. The observation period until all mice became moribund or died was 1,195 days for females and 1,217 days for males. However, there was no significant difference between males and females during the observation period.

A Cox regression approach was used to calculate the hazard ratio for the development of lung lesions for each radiation type and dose, resulting in linear-dose-response curves for lung AD in neutron-irradiated female mice and for lung AC in gamma-irradiated, carbon-ion irradiated, or neutron-irradiated male and female mice (Tables 2–4 and Fig. 2). An approximation curve could be obtained except for the hazard ratio calculated for 4 Gy gamma irradiation owing to the small sample size (Fig. 2D). In fact, the linear fit was improved by excluding the value for 4 Gy gamma irradiation [see Akaike's information criterion/AIC values (Table 5)]. RBE values for the development of lung lesions were then calculated using the hazard ratio data. The RBEs for carbon-ion and neutron irradiation with respect to lung AC development were 1.07 and 4.78 for males and 2.59 and 4.57 for females, respectively (Table 1). These data suggested that the effect of carbon ions (LET of 13 keV/μm) for lung AC development was similar to that of gamma rays and that the effect of neutrons (mean energy, ~2 MeV) was approximately 4- to 5-fold greater than that of gamma rays.

Genetic Alterations in Lung ACs of Irradiated Mice

To investigate changes in genomic copy number in mouse lung ACs that developed either spontaneously or after irradiation, we performed array-CGH analysis of the tumors. Tumors from all groups had frequent DNA copy-number losses in chromosome 4 and gains in chromosome 6 (Supplementary Fig. S3A; https://doi.org/10.1667/RADE-21-00192.1.S2). To identify genes affected by the copy-number alterations, LOH was assessed using satellite markers located in chromosomes 4 and 6. LOH and allelic imbalance were frequently observed proximal to the tumor-suppressor gene *Cdkn2b* in chromosome 4, whereas allelic imbalance was frequently observed proximal to the oncogenes *Braf* and *Kras* in chromosome 6 (Supplementary Fig. S3B; https://doi.org/10.1667/RADE-21-00192.1.S2). Kras is involved in Egfr signaling, the disruption of which contributes to lung-cancer development (*26*). The Egfr signaling pathway is the most frequently mutated oncogenic pathway in human lung AC (*27*). Among the genes involved in this pathway, *Trp53*, *Cdkn2b*, *Kras* and *Braf* are most frequently mutated (*27*). We thus analyzed somatic mutations in these genes. Somatic mutations in *Kras* and *Braf* were detected in 29% (7 of 24) and 8% (2 of 24) of tumors, respectively, whereas no mutations were detected in *Trp53* or *Cdkn2b* (Supplementary Table S2; https://doi.org/10.1667/RADE-21-00192.1.S1 and Supplementary Fig. S4; https://doi.org/10.1667/RADE-21-00192.1.S2). These find-

TABLE 3
Hazard Ratio Values for the Development of Lung Lesions after Irradiation of Mice with Carbon Ions

Sex	Lung lesion	Dose (Gy)	No. of animals	P value	Hazard ratio	95% CI Lower limit	95% CI Upper limit
Male	Adenoma	0	111	0.20	1.00	-	-
		0.2	43	0.09	0.27	0.06	1.20
		0.5	40	0.18	0.36	0.08	1.62
		1	40	0.44	1.56	0.50	4.90
		2	41	0.29	1.88	0.59	5.97
		4	40	0.97	1.05	0.13	8.31
	Adenocarcinoma	0	111	0.00	1.00	-	-
		0.2	43	0.63	1.27	0.48	3.36
		0.5	40	0.59	0.70	0.19	2.57
		1	40	0.26	2.17	0.57	8.28
		2	41	<0.001***	6.83	2.51	18.58
		4	40	<0.001***	11.40	3.68	35.34
Female	Adenoma	0	108	0.94	1.00	-	-
		0.2	36	0.76	1.22	0.31	4.78
		0.5	41	0.26	2.20	0.54	8.88
		1	41	0.85	1.16	0.24	5.67
		2	48	0.98	0.91	0.11	7.63
		4	40	0.99	0.00	0.00	-
	Adenocarcinoma	0	108	0.01	1.00	-	-
		0.2	36	0.16	2.72	0.68	10.92
		0.5	41	0.33	2.30	0.42	12.62
		1	41	0.016*	4.98	1.34	18.58
		2	48	0.002**	9.08	2.53	32.54
		4	40	0.001**	14.61	3.17	67.44

Notes. CI = confidence interval; $P < 0.05$; $^{**}P < 0.01$; $^{***}P < 0.001$ vs. no irradiation.

TABLE 4
Hazard Ratio Values for the Development of Lung Lesions after Irradiation of Mice with Neutrons

Sex	Lung lesion	Dose (Gy)	No. of animals	P value	Hazard ratio	95% CI Lower limit	95% CI Upper limit
Male	Adenoma	0	111	0.41	1.00	-	-
		0.05	49	0.17	0.35	0.08	1.54
		0.1	50	0.22	1.85	0.70	4.93
		0.2	50	0.86	1.11	0.36	3.42
		0.5	50	0.36	1.83	0.51	6.59
		1	50	0.56	1.57	0.35	7.09
	Adenocarcinoma	0	111	0.00	1.00	-	-
		0.05	49	0.09	2.17	0.88	5.33
		0.1	50	0.94	1.05	0.29	3.87
		0.2	50	0.034*	2.77	1.08	7.13
		0.5	50	0.024*	3.37	1.17	9.69
		1	50	<0.001***	6.41	2.49	16.51
Female	Adenoma	0	108	0.06	1.00	-	-
		0.05	50	0.48	1.65	0.41	6.62
		0.1	50	0.44	0.44	0.05	3.57
		0.2	50	0.32	2.03	0.51	8.13
		0.5	50	0.23	2.76	0.54	14.21
		1	50	0.004**	9.92	2.13	46.29
	Adenocarcinoma	0	108	0.00	1.00	-	-
		0.05	50	0.62	1.54	0.28	8.41
		0.1	50	0.07	3.34	0.90	12.45
		0.2	50	0.027*	4.42	1.18	16.51
		0.5	50	0.64	1.71	0.19	15.70
		1	50	0.005**	9.62	1.96	47.30

Notes. CI = confidence interval; $^{*}P < 0.05$; $^{**}P < 0.01$; $^{***}P < 0.001$ *vs.* no irradiation.

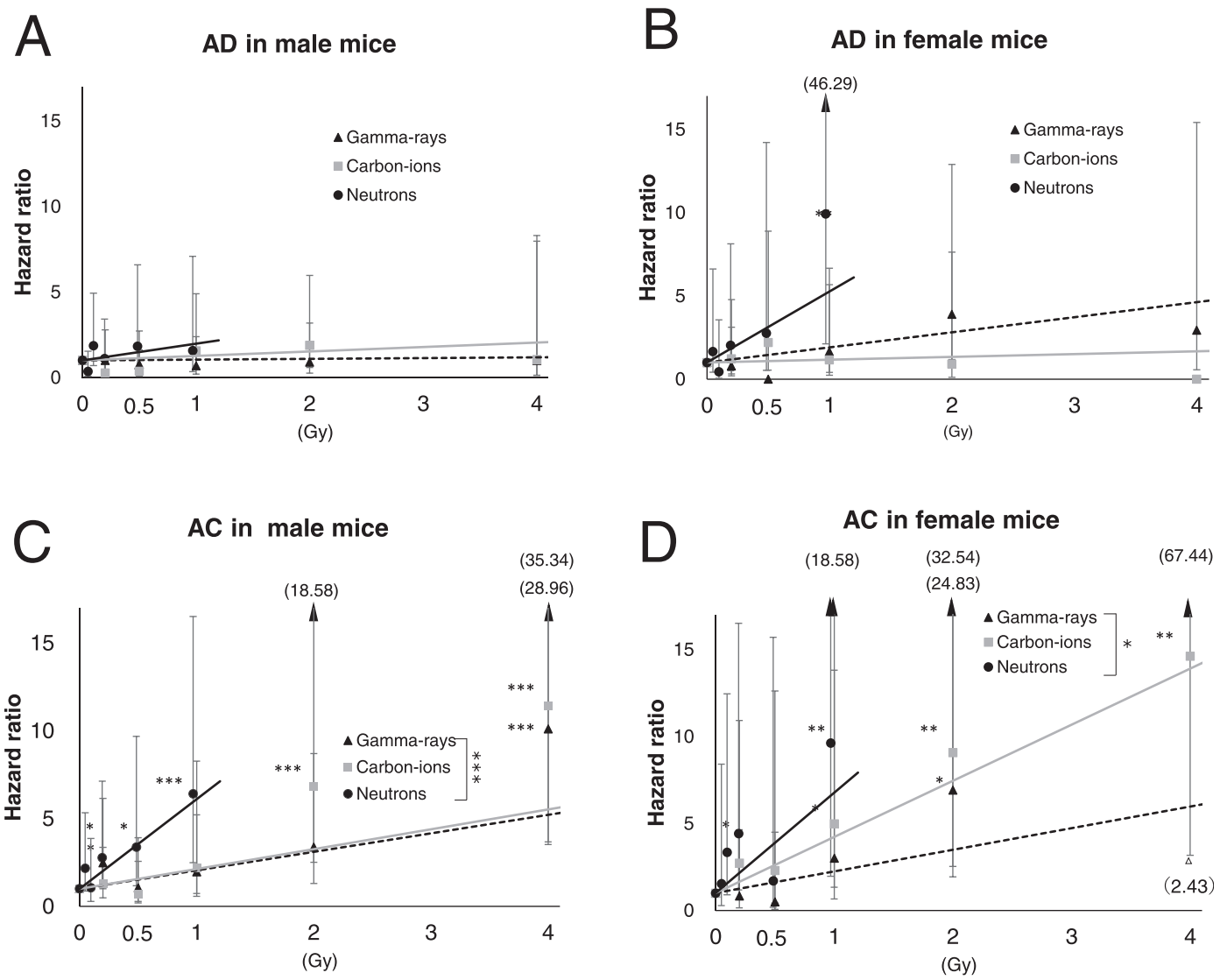

FIG. 2. Cox proportional hazard analysis of lung lesions in irradiated mice. The hazard ratio for the development of lung AD or AC in male (panels A and C) and female (panels B and D) mice is plotted against radiation dose. Vertical bars indicate the 95% confidence interval. Linear fitting was performed by the least-squares method, and the corresponding Akaike's information criterion (AIC) value is indicated in Table 5. *P $<$ 0.05, **P $<$ 0.01 and ***P $<$ 0.001 vs. no irradiation.

TABLE 5
RBE Values for Carbon Ions and Neutrons for Lung-Tumor Development

		Slope			RBE (95% CI)		AIC[a]	
Sex	Lung lesion	Gamma rays	Carbon ions	Neutrons	Carbon ions	Neutrons	L model[b]	LQ model[c]
Male	Adenoma	0.045	0.26	0.98	5.79 (2.23 × 10^{-4}, 1.5 × 10^{5})	22.12 (7.91 × 10^{-4}, 6.19 × 10^{5})	**596.41**	597.72
	Adenocarcinoma	1.05	1.13	5.10	1.07 (0.45, 2.60)	4.78 (2.02, 11.32)	**1112.65**	1113.76
Female	Adenoma	0.91	0.17	4.26	0.18 (3.16 × 10^{-4}, 109.17)	4.63 (0.89, 24.08)	396.13	**394.15**
	Adenocarcinoma	1.24	3.22	5.77	2.59 (0.84, 8.04)	4.57 (1.14, 18.28)	**611.42**	612.91

Notes. RBE, relative biological effectiveness. The values of slope and RBE shown in the table were calculated based on the Linear model.
[a] Akaike's information criterion; the smallest value (indicated in boldface type) indicates the best model.
[b,c]Linear model, 1 + αD; linear-quadratic model, 1 + αD + βD^2, where D is dose.

ings suggested that alterations in genes involved in Egfr signaling are common in both spontaneous and radiation-induced lung tumors.

Activation of the Egfr Pathway in Lung Lesions of Irradiated Mice

To examine the activation of the Egfr pathway in lung lesions that developed spontaneously or after irradiation, we performed immunohistochemical staining for Erk and its activated form (phospho-Erk) in tumor-tissue samples. Erk was present in all lung-tumor tissues (Fig. 3A). No dose-dependent changes in p-Erk positivity were observed for any radiation type, regardless of AD, AC, or gender. This may be attributable to the small sample size. Interestingly, lung ADs and ACs from the irradiated groups were intensely immunostained for phospho-Erk compared with the non-irradiated group (Fig. 3B–E). Intense phospho-Erk immunostaining was frequently observed in lung ACs from the carbon-ion irradiated or neutron-irradiated groups compared with ACs from the gamma-ray-irradiated group (Fig. 3D and E). For the irradiated groups, the frequency of intense phospho-Erk immunostaining was also greater in ACs than ADs. With regard to the between-group comparisons, significant differences in the positivity rate were observed for carbon-ion irradiated and neutron-induced ACs in males ($P < 0.001$ and $P = 0.025$) and for gamma-ray-induced ACs in females ($P = 0.036$) compared with spontaneous tumor development. These findings indicated that Egfr signaling is activated in both spontaneous and radiation-induced lung cancers, and this signaling is further upregulated in radiation-induced tumors.

Presence of Nuclear Grooves in Lung Lesions of Irradiated Mice

Cells from mouse lung tumors also displayed a nuclear abnormality referred to as ''nuclear grooves'' (Fig. 4A), which are longitudinal invaginations of the nuclear envelope bilayer (*28*). No dose-dependent change in the positivity rate of nuclear grooves was apparent for any radiation type, regardless of AD, AC, or gender, which may be attributable to the small sample size. However, the frequency of nuclear grooves was greater in ACs than ADs (Fig. 4B–E). For the between-group comparison, the positivity rate for carbon-ion induced ACs in males differed significantly from that of the spontaneous group ($P < 0.001$) (Fig. 4D). Notably, ACs from the irradiated groups had a particularly high frequency of nuclear grooves, suggesting a histopathological difference between radiation-induced and spontaneously developed lung cancers.

DISCUSSION

With the increased use of modern radiotherapy techniques for cancer treatment, there is a growing concern about the risk of developing a secondary cancer. Although fractionated irradiation is often used in radiotherapy, initially we focused on the effect of acute irradiation as a basis for assessing the risk of developing secondary cancer. We evaluated the risk of developing lung AC in male and female mice exposed to carbon ions (LET 13 keV/μm) or fast neutrons (mean energy, ~2 MeV). As shown in Table 5, the RBE values for carbon ions for lung AC development were 1.07 and 2.59 for male and female mice, respectively; in contrast, the corresponding values for neutrons were 4.63 and 4.57. Although RBE values can vary widely depending on the endpoint, these RBE values for carbon ions are consistent with reported values (range, ~1 to 2) having the same energy and LET for different endpoints, such as chromosome aberrations, damage to normal tissues, and tumor response (*29*).

Conversely, based on tumor incidence, the RBE values for lung AC development in SAS/4 mice irradiated with fast neutrons (mean energy of 7.5 MeV) at 12 weeks or in B6CF1 mice irradiated with fission neutrons (0.86 MeV) at 12 weeks have been reported as follows: male, 4.5 or 9.2; female, 7.4 or 13.0, respectively (*30, 31*). In addition, very high-RBE values (e.g., 18.5) have been reported in fission neutron-radiation experiments using female Balb/c mice at 12 weeks of age (*32, 33*). These values are greater than those obtained in our present study, and this may reflect differences in the energy of neutrons, mouse strain or age, or methods for RBE calculation (*17, 30, 34, 35*). Using RFM mice irradiated at 12 weeks of age, Ullrich et al. also reported the lack of a dose-response relationship for the incidence of lung cancer, resulting in the failure of the RBE calculation (*36*). Although our RBE value for carbon ions for AC development was higher in female mice than in males, the RBE value for neutrons for AC development was not greater for female mice than males. However, when comparing the slopes of the approximation curves in the hazard analysis of lung AC, the hazard for carbon-ion and neutron exposure for female mice tended to be greater than that for males (Fig. 2 and Table 5). This is attributable to the lower incidence of spontaneously developing lung tumors and higher induction of lung tumors after irradiation of

→

FIG. 3. Hyperactivation of the Egfr pathway in lung lesions of irradiated mice. Panel A: Representative histological images for hematoxylin and eosin (HE) staining as well as Erk and phospho-Erk immunostaining of lung AC tissue. Images show lung ACs with negative (–), positive (+), or strong positive (++) phospho-Erk staining. Frequency of phospho-Erk-negative and -positive lung AD and AC in male (panels B and D) and female (panels C and E) mice in the non-irradiated mouse group as well as groups irradiated with gamma rays, carbon ions, or neutrons. Scale bar, 100 μm. *$P < 0.05$ and ***$P < 0.001$ vs. no irradiation.

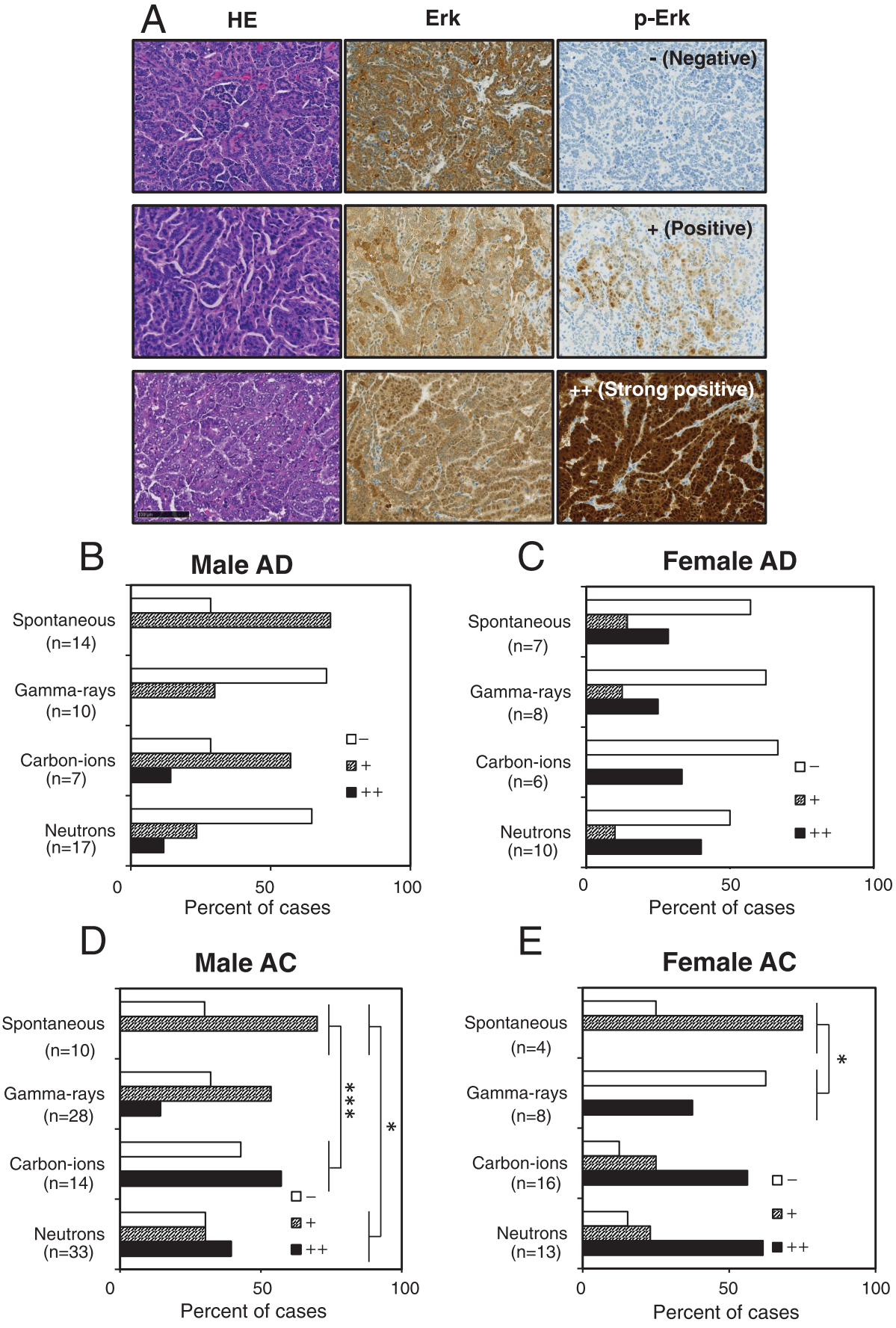

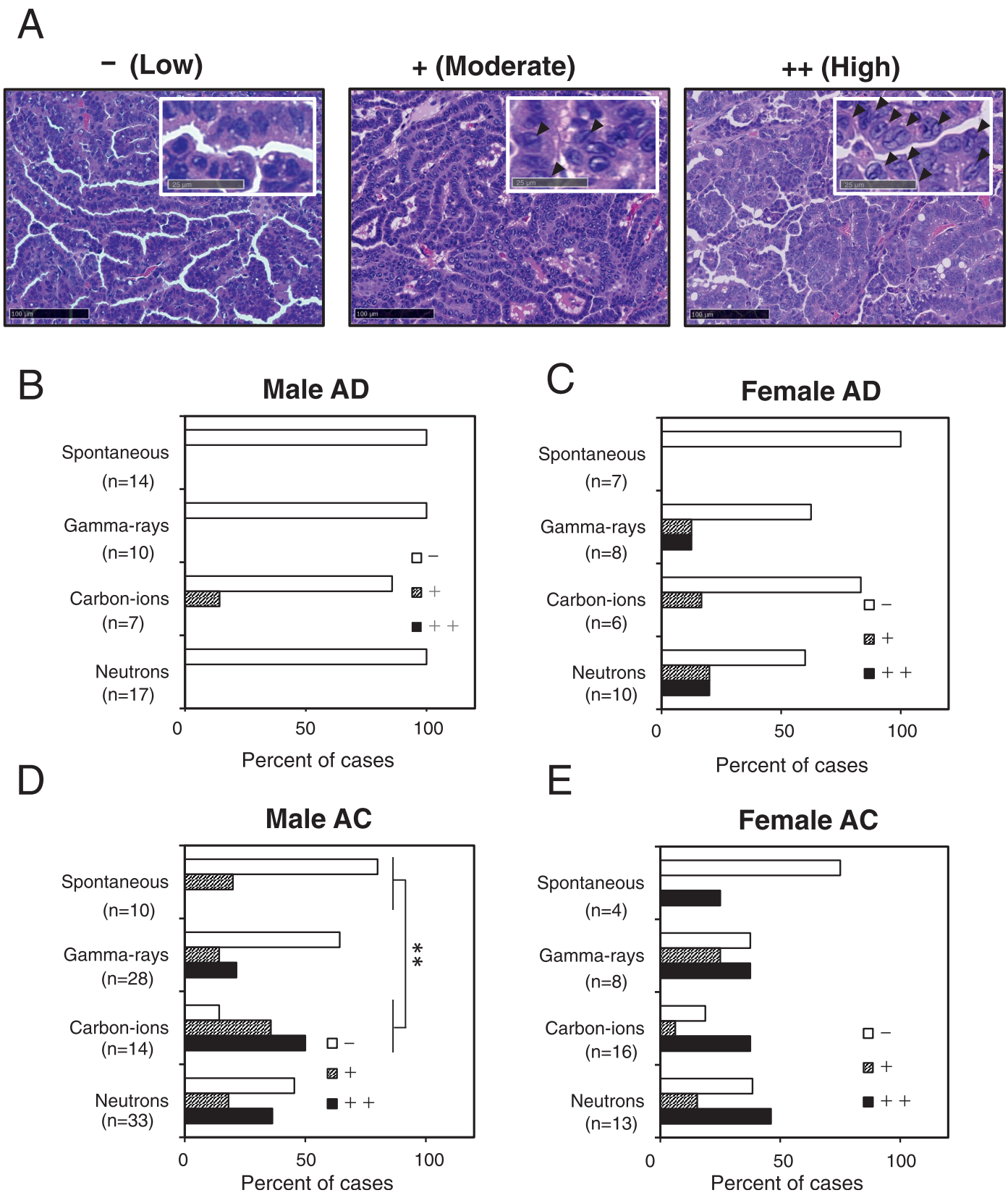

FIG. 4. Frequency of nuclear grooves in lung lesions of irradiated mice. Panel A: Representative histological images of lung AC tissue with nuclear grooves. Images show lung ACs with low (–), moderate (+), or high (++) incidence of nuclear grooves. Nuclear grooves are indicated by arrowheads in each inset. Panels B–E: Frequency of nuclear grooves in lung AD and AC of male (panels B and D) and female (panels C and E) mice. Scale bars, 100 μm. Insets show high-magnification images (scale bars, 25 μm). **$P < 0.01$ vs. no irradiation.

female mice compared with males (Tables 1–4), and this trend is consistent with previous reports (*30, 31*). In this regard, a higher lung-cancer risk for women after radiation exposure has been reported in epidemiological studies of Japanese atomic-bomb survivors and Russian Mayak workers with a lower background incidence and higher radiation-induced lung cancer in women than men in both cohorts (*37, 38*). Subsequent studies have found that the difference in risk between women and men becomes significantly smaller when corrected for the prevalence of tobacco smoking (*37, 38*). However, a recent study showed an interaction between moderate tobacco use and radiation exposure with respect to a higher risk of lung cancer in woman (*15*). The exact reason for this discrepancy between the mouse and human studies is not clear, but it may be attributable to differences in the age distribution in the populations studied because, although the mice were exposed at a uniform age, the epidemiological cohorts included populations who were exposed to ionizing radiation at a wide range of ages. In addition, studies using different mouse strains (including B6CF1, Balb/C, RFM, and SAS/4 mice) suggest an important genetic dependency on lifestyle factors such as tobacco use, among other factors (*30–32, 36*).

We observed frequent DNA copy-number losses in chromosome 4 and gains in chromosome 6 as well as mutations in genes involved in Egfr signaling in lung ACs from both non-irradiated and irradiated mice (Supplementary Fig. S3; https://doi.org/10.1667/RADE-21-00192.1.S2 and Supplementary Table S2; https://doi.org/10.1667/RADE-21-00192.1.S1). Consistent with our findings, Hegi et al. reported changes in DNA copy number in chromosomes 4 and 6 in mouse lung ACs induced by a chemical carcinogen (*39*). Concerning the results for chromosome 4, deletions have also been reported in a putative tumor-suppressor gene in chemically induced or spontaneous mouse lung tumors (*40*). Similarly, frequent point mutations in *Kras* (chromosome 6) have been found in radiation-induced lung ACs in mice (*19*). The Egfr/Kras signaling axis is the most frequently mutated pathway in human lung ACs (*27, 41*). These observations suggest that mutation/disruption of Egfr signaling is common in radiation-induced lung tumorigenesis.

Activation of Egfr signaling leads to the hyperphosphorylation of Erk-family MAP kinases (*42*). Our present study revealed frequent, intense phospho-Erk immunostaining in lung ACs of mice irradiated with carbon ions or neutrons compared with ACs from the non-irradiated or gamma-ray-irradiated groups (Fig. 3). Notably, hyperphosphorylation of Erk correlates with an increased rate of cancer progression, including lung cancers (*43*). Iron-ion irradiation of a K-rasLA1 mouse model reportedly increases the incidence of lung cancer (*44*), indicating the involvement of K-ras/Erk signaling in high-LET radiation-induced lung cancer. This suggests that malignant lung ACs induced by high-LET radiation reduce overall survival more so than do ACs induced by gamma rays (Fig. 1). In addition, concerning the greater hazard for female mice than males (Fig. 2 and Table 5), it should be noted that intense phospho-Erk immunostaining was more frequently observed in lung ACs of females irradiated with carbon ions or neutrons compared with similarly irradiated males (Fig. 3E).

We also found that, in comparison with spontaneous ACs, a large proportion of mouse lung ACs from the irradiated groups, particularly the high-LET group, had nuclear grooves (Fig. 4B–E). Indeed, nuclear grooves have also been found in human lung tumors (*45, 46*), and thus nuclear grooves may be one of the characteristics of radiation-induced lung-tumor cells.

Our findings provide valuable information for assessing the risk of developing lung tumors after patients receive particle-beam therapy and enhance our understanding of the molecular basis of tumorigenesis.

SUPPLEMENTARY MATERIALS

Supplementary Table S1. Primer sequences and PCR conditions for the mutation analysis.

Supplementary Table S2. *Braf*, *Kras* and *Egfr* mutations in radiation-induced lung adenocarcinomas.

Supplementary Fig. S1. Incidence of lung AD in irradiated mice. Kaplan-Meier curves for lung AD-free survival of male and female mice after irradiation with 0.2–4 Gy of gamma rays (panels A and B) or carbon ions (panels C and D) or 0.05–1 Gy of neutrons (panels E and F). Data for non-irradiated control mice are also presented. *P $<$ 0.05, ***P $<$ 0.001 vs. no irradiation.

Supplementary Fig. S2. Incidence of lung AC in irradiated mice. Kaplan-Meier curves for lung AC-free survival of male and female mice after irradiation with 0.2–4 Gy of gamma rays (panels A and B) or carbon ions (panels C and D) or 0.05–1 Gy of neutrons (panels E and F). Data for non-irradiated control mice are also presented. *P $<$ 0.05, **P $<$ 0.01 and ***P $<$ 0.01 vs. no irradiation.

Supplementary Fig. S3. Genetic alterations in lung ACs of irradiated mice. Panel A: Genome-wide view of array-CGH data for lung ACs (n = 24). The frequency (%) is indicated for amplifications (red) and losses (green) in all tumors analyzed. Panel B: DNA copy number and LOH on chromosomes 4 and 6 in lung ACs from non-irradiated mice as well as mice irradiated with gamma rays, carbon ions, or neutrons. Arrows indicate the locations of the genes *Cdkn2b*, *Braf* and *Kras*. Polymorphic markers and their positions are shown in the chromosome schematic. Closed circles represent LOH, open circles represent F1, and closed triangles represent allelic imbalance.

Supplementary Fig. S4. Egfr pathway gene mutations in lung ACs. The Egfr signaling pathway is shown along with mutation frequencies for *Kras*, *Braf*, *Trp53* and *Cdkn2b* identified in lung ACs. The numbers in parentheses indicate the number of mutations found in the 24 samples investigated. Pi3k: phosphatidylinositol 3-kinase.

ACKNOWLEDGMENTS

We thank all members of the Department of Radiation Effects Research for their technical and secretarial assistance, and to all members of the Division of Animal Facility for help with animal maintenance. This study was supported in part by Grants-in-Aid for Scientific Research from the Ministry of Education, Culture, Sports, Science, and Technology of Japan (No. 19K20454 to K. Suzuki, and No. JP15K16549 to S. Yamazaki), by an institutional grant from NIRS (to K. Iwata), and by QST Diversity Promotion Grant (to K. Suzuki).

Received: October 5, 2021; accepted: July 25, 2022; published online: August 30, 2022

REFERENCES

1. De Ruysscher D, Mark Lodge M, Jones B, Brada M, Munro A, Jefferson T, et al. Charged particles in radiotherapy: a 5-year update of a systematic review. Radiother Oncol 2012; 103, 5-7.
2. Imaoka T, Nishimura M, Daino K, Takabatake M, Moriyama H, Nishimura Y, et al. Risk of second cancer after ion beam radiotherapy: insights from animal carcinogenesis studies. Int J Radiat Biol 2019; 95, 1431-40.
3. Kanai T, Endo M, Minohara S, Miyahara N, Koyama-ito H, Tomura H, et al. Biophysical characteristics of HIMAC clinical irradiation system for heavy-ion radiation therapy. Int J Radiat Oncol Biol Phys 1999; 44, 201-10.
4. Dang B, Li W, Wang J, Comparison doses of secondary neutron with the heavy ions in a 75-Mev/n heavy ion beam. Radiat Prot Dosimetry 2005; 117, 369-72.
5. Schneider U, Agosteo S, Pedroni E, Besserer J, Secondary neutron dose during proton therapy using spot scanning. Int J Radiat Oncol Biol Phys 2002; 53, 244-51.
6. Jemal A, Siegel R, Ward E, Murray T, Xu J, Smigal C, et al. Cancer statistics, 2006. CA Cancer J Clin 2006; 56, 106-30.
7. Group GBDNDC, Global, regional, and national burden of neurological disorders during 1990-2015: a systematic analysis for the Global Burden of Disease Study 2015. Lancet Neurol 2017; 16, 877-97.
8. Furukawa K, Preston DL, Lonn S, Funamoto S, Yonehara S, Matsuo T, et al. Radiation and smoking effects on lung cancer incidence among atomic bomb survivors. Radiat Res 2010; 174, 72-82.
9. Preston DL, Ron E, Tokuoka S, Funamoto S, Nishi N, Soda M, et al. Solid cancer incidence in atomic bomb survivors: 1958-1998. Radiat Res 2007; 168, 1-64.
10. United Nations Scientific Committee on the Effects of Atomic Radiation (2012) Sources, and Effects of Ionizing Radiation. UNSCEAR 2012 Report. UNSCEAR
11. Darby S, Whitley E, Silcocks P, Thakrar B, Green M, Lomas P, et al. Risk of lung cancer associated with residential radon exposure in south-west England: a case-control study. Br J Cancer 1998; 78, 394-408.
12. Lane RSD, Tomasek L, Zablotska LB, Rage E, Momoli F, Little J, Low radon exposures and lung cancer risk: joint analysis of the Czech, French, and Beaverlodge cohorts of uranium miners. Int Arch Occup Environ Health 2019; 92, 747-62.
13. Grantzau T, Thomsen MS, Vaeth M, Overgaard J, Risk of second primary lung cancer in women after radiotherapy for breast cancer. Radiother Oncol 2014; 111, 366-73.
14. Land CE, Shimosato Y, Saccomanno G, Tokuoka S, Auerbach O, Tateishi R, et al. Radiation-associated lung cancer: a comparison of the histology of lung cancers in uranium miners and survivors of the atomic bombings of Hiroshima and Nagasaki. Radiat Res 1993; 134, 234-43.
15. Egawa H, Furukawa K, Preston D, Funamoto S, Yonehara S, Matsuo T, et al. Radiation and smoking effects on lung cancer incidence by histological types among atomic bomb survivors. Radiat Res 2012; 178, 191-201.
16. D. Grahn BJW, B. A. Carnes, F. S. Williamson and C. Fox, Studies of Acute and Chronic Radiation Injury at the Biological and Medical Research Division, Argonne National Laboratory, 1970-1992: The JANUS Program Survival and Pathology Data. 1995.
17. Storer JB, Mitchell TJ, Fry RJ, Extrapolation of the relative risk of radiogenic neoplasms across mouse strains and to man. Radiat Res 1988; 114, 331-53.
18. Zhang Y, Woloschak GE, Rb and p53 gene deletions in lung adenocarcinomas from irradiated and control mice. Radiat Res 1997; 148, 81-9.
19. Zhang Y, Woloschak GE, Detection of codon 12 point mutations of the K-ras gene from mouse lung adenocarcinoma by 'enriched' PCR. Int J Radiat Biol 1998; 74, 43-51.
20. Morioka T, Blyth BJ, Imaoka T, Nishimura M, Takeshita H, Shimomura T, et al. Establishing the Japan-Store house of animal radiobiology experiments (J-SHARE), a large-scale necropsy and histopathology archive providing international access to important radiobiology data. Int J Radiat Biol 2019; 95, 1372-77.
21. Wang TJ, Wu CC, Chai Y, Lam RK, Hamada N, Kakinuma S, et al. Induction of non-targeted stress responses in mammary tissues by heavy ions. PLoS One 2015; 10, e0136307.
22. Takada M SM, Kamada S, Hagiwara T, Imaseki H, Hamano T., Neutron Exposure Accelerator System for Biological Effect Experiments (NASBEE). AIP Conference Proceedings 2011, 401-5.
23. Yonai S, Matsufuji N, Kanai T, Matsui Y, Matsushita K, Yamashita H, et al. Measurement of neutron ambient dose equivalent in passive carbon-ion and proton radiotherapies. Med Phys 2008; 35, 4782-92.
24. Masashi Takada MS, So Kamada, Takuya Hagiwara, Hitoshi Imaseki, and Tsuyoshi Hamano, Neutron Exposure Accelerator System for Biological Effect Experiments (NASBEE). AIP Conference Proceedings 2011; 401, 1336.
25. R: RCT, A language and environment for statistical computing. Vienna: R Foundation for Statistical Computing. 2013. (https://www.r-project.org/).
26. Shigematsu H, Gazdar AF, Somatic mutations of epidermal growth factor receptor signaling pathway in lung cancers. Int J Cancer 2006; 118, 257-62.
27. Cancer Genome Atlas Research N, Comprehensive molecular profiling of lung adenocarcinoma. Nature 2014; 511, 543-50.
28. Batistatou A, Scopa CD, Pathogenesis and diagnostic significance of nuclear grooves in thyroid and other sites. Int J Surg Pathol 2009; 17, 107-10.
29. Ando K, Kase Y, Biological characteristics of carbon-ion therapy. Int J Radiat Biol 2009; 85, 715-28.
30. Coggle JE, Lung tumour induction in mice after X-rays and neutrons. Int J Radiat Biol Relat Stud Phys Chem Med 1988; 53, 585-97.
31. Heidenreich WF, Carnes BA, Paretzke HG, Lung cancer risk in mice: analysis of fractionation effects and neutron RBE with a biologically motivated model. Radiat Res 2006; 166, 794-801.
32. Ullrich RL, Tumor induction in BALB/c female mice after fission neutron or gamma irradiation. Radiat Res 1983; 93, 506-15.
33. Ullrich RL, Tumor induction in BALB/c mice after fractionated or protracted exposures to fission-spectrum neutrons. Radiat Res 1984; 97, 587-97.
34. Zacharatou Jarlskog C, Paganetti H, Risk of developing second cancer from neutron dose in proton therapy as function of field characteristics, organ, and patient age. Int J Radiat Oncol Biol Phys 2008; 72, 228-35.
35. Shuryak I, Sachs RK, Brenner DJ, Cancer risks after radiation exposure in middle age. J Natl Cancer Inst 2010; 102, 1628-36.

36. Ullrich RL, Jernigan MC, Adams LM, Induction of lung tumors in RFM mice after localized exposures to X rays or neutrons. Radiat Res 1979; 80, 464-73.

37. Cahoon EK, Preston DL, Pierce DA, Grant E, Brenner AV, Mabuchi K, et al. Lung, Laryngeal and Other Respiratory Cancer Incidence among Japanese Atomic Bomb Survivors: An Updated Analysis from 1958 through 2009. Radiat Res 2017; 187, 538-48.

38. Sokolnikov ME, Gilbert ES, Preston DL, Ron E, Shilnikova NS, Khokhryakov VV, et al. Lung, liver and bone cancer mortality in Mayak workers. Int J Cancer 2008; 123, 905-11.

39. Hegi ME, Devereux TR, Dietrich WF, Cochran CJ, Lander ES, Foley JF, et al. Allelotype analysis of mouse lung carcinomas reveals frequent allelic losses on chromosome 4 and an association between allelic imbalances on chromosome 6 and K-ras activation. Cancer Res 1994; 54, 6257-64.

40. Herzog CR, Wiseman RW, You M, Deletion mapping of a putative tumor suppressor gene on chromosome 4 in mouse lung tumors. Cancer Res 1994; 54, 4007-10.

41. Slebos RJ, Kibbelaar RE, Dalesio O, Kooistra A, Stam J, Meijer CJ, et al. K-ras oncogene activation as a prognostic marker in adenocarcinoma of the lung. N Engl J Med 1990; 323, 561-5.

42. Cobb MH, MAP kinase pathways. Prog Biophys Mol Biol 1999; 71, 479-500.

43. Vicent S, Lopez-Picazo JM, Toledo G, Lozano MD, Torre W, Garcia-Corchon C, et al. ERK1/2 is activated in non-small-cell lung cancer and associated with advanced tumours. Br J Cancer 2004; 90, 1047-52.

44. Delgado O, Batten KG, Richardson JA, Xie XJ, Gazdar AF, Kaisani AA, et al. Radiation-enhanced lung cancer progression in a transgenic mouse model of lung cancer is predictive of outcomes in human lung and breast cancer. Clin Cancer Res 2014; 20, 1610-22.

45. Choi IH, Kim DW, Ha SY, Choi YL, Lee HJ, Han J, Analysis of Histologic Features Suspecting Anaplastic Lymphoma Kinase (ALK)-Expressing Pulmonary Adenocarcinoma. J Pathol Transl Med 2015; 49, 310-7.

46. Kobayashi S, Saio M, Fukuda T, Kimura K, Hirato J, Oyama T, Image analysis of the nuclear characteristics of emerin protein and the correlation with nuclear grooves and intranuclear cytoplasmic inclusions in lung adenocarcinoma. Oncol Rep 2019; 41, 133-42.